RESEARCH ARTICLE

Two-Dimensional Switchable Beam Transmitarray Antenna for mm-Wave Base Stations and Vehicular Networks

JAVID AHMAD GANIE [ID], (Graduate Student Member, IEEE),
AND KUSHMANDA SAURAV [ID], (Member, IEEE)

Department of Electrical Engineering, Indian Institute of Technology Jammu, Jammu, Jammu and Kashmir 181221, India

Corresponding author: Javid Ahmad Ganie (khosajavid1263@gmail.com)

ABSTRACT This article presents the design of a low-profile, two-dimensional and beam-switching transmitarray antenna for millimetre-wave (26.3-29.3 GHz) applications. The transmitarray panel is designed using two substrate layer polarization rotating phase shift elements. The phase distribution on the transmitarray panel is approximated by 0 and π. The phase shift element dimensions are $0.22\lambda_0$ x $0.22\lambda_0$ x $0.14\lambda_0$, (λ_0 corresponds to frequency of 28 GHz). The overall size of the transmitarray panel is 5.6 λ_0 x 5.6 λ_0 with a focus-to-dimension (f/d) ratio of 0.5, which makes the design compact. The panel is fed by a 9-port Yagi array antenna arranged in a 3×3 configuration. The offset antennas undergo a scanning loss of 1.6 dB with a peak gain of 19.7 dBi in the main beam. The 3-dB beamwidth of 9.8-11.2° is obtained in different radiation beams. The radiation patterns of the offset antennas are tilted $\pm 15°$ with respect to the focal antenna, thus giving a radiation coverage of 30°. The antenna can be used in millimetre wave base stations for beam-switching and can also act as a repeater antenna at millimetre wave frequencies in public transport vehicles.

INDEX TERMS Beam-switching, beamforming, two dimensional, phase-shift elements, transmitarray.

I. INTRODUCTION

The future 5G wireless communication applications have a data rate requirement of at least 10-50 Gb/s [1]. This data rate requirement is ten times higher than the LTE-A peak data rate. Due to spectral congestion in the sub-6 GHz bands, researchers in academia and industry hunt for hardware design at millimetre-wave frequencies, which provide higher data rates. The IEEE 802.15.3.c-2009, a current millimetre-wave standard, provides a 2-9 GHz bandwidth. This bandwidth is 20 times larger than the average bandwidth of LTE-A Pro [2]. Due to high data rates, high resolution and the small hardware size at millimetre wave frequencies, the radar systems at mm-wave frequencies can help in building wireless communication links for vehicles and unmanned aerial vehicles (UAV) [3] (Fig. 1(a)).

The associate editor coordinating the review of this manuscript and approving it for publication was Mohammed Bait-Suwailam [ID].

The main shortcomings at the mm-wave frequencies are the high propagation loss, rain-fade and high penetration loss which severely attenuate the signal while encountering blockages over long distances [4]. The penetration losses >20dB have been found at 28GHz for concrete and bricks [5]. The solution to this problem is using high gain antennas at mm-wave frequencies, compensating for the high propagation loss [6], [7], [8], [9]. However, the high-gain antennas necessarily mean low beamwidth, which leads to poor coverage. As the number of users is expected to grow exponentially in the future 5G communications, each user requires a highly directive radiation beam for smooth and hassle-free communication. The multi-beam antennas capable of generating a number of independent high directive beams and covering a wide angular range provide a stable communication link at mm-wave frequencies for vehicular or mobile networks [10], [11], [12], [13], [14], [15]. The penetration losses of mm-waves will be very high if the passengers
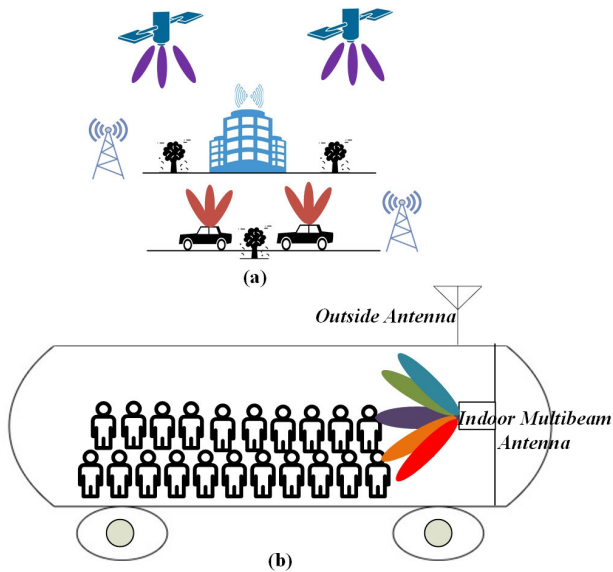
FIGURE 1. Application scenario of the 5G millimetre wave communication in vehicular networks.

FIGURE 2. Schematic of a generalized transmitarray antenna.

travelling on public transport communicate directly with the base stations. This problem can be solved by using a single antenna at the rooftop of the vehicle and a high-gain multi-beam antenna inside the moving vehicle [16] (Fig.1(b)). The indoor multi-beam antenna can provide a hassle-free communication link to the passengers.

In literature, various beamforming prototypes using active phase shifters are reported [17], [18], [19], [20], [21] to validate the performance at mm-wave frequencies. A 8×4 uniform planar array antenna is used along with phase shifters and mixers in [17] to demonstrate the analogue beamforming at 27.925 GHz. The phase shifter-based 3-D hybrid beamforming prototype at millimetre-wave is presented in [18]. A 29 GHz hybrid beamforming IC, using phase shifters and a 2×2 patch antenna, is presented in [19]. The primary purpose of beamforming reported in [16], [17], and [18] is to direct the radiation beams in different directions to multiple users. The reported modelling and design approach can be extended to a huge number of antennas to increase the system's coverage. The preceding prototypes demonstrated that beamforming is suitable for mm-wave communication. However, the use of active circuitry leads to high power consumption, which makes these designs energy inefficient. Furthermore, the hardware design complexity associated with these prototypes makes the designs mentioned above challenging to implement.

A lens antenna can be used in place of a conventional phase shifter in the beamforming to cut down the power consumption and reduce the design complexity [3], [6], [22], [23], [24], [25], [26], [27], [28]. The energy-focusing property of the lens antenna can be used to direct a highly directive beam in a particular direction [29]. MIMO antennas combined with the lens antenna are energy-efficient hardware to implement the beamforming at mm-wave frequencies. It reduces
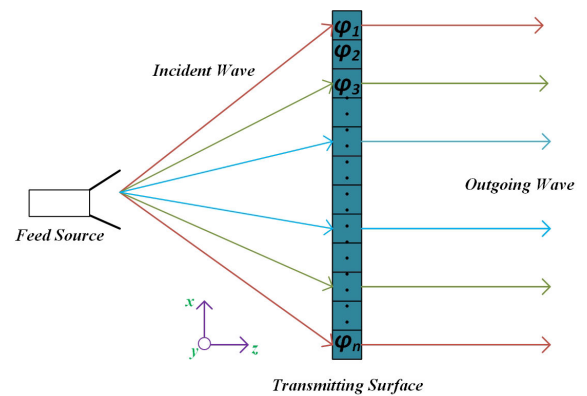
power consumption, reduces design complexity, and makes the beam directive. The MIMO antennas integrated with the lens antenna also curtail the signal processing complexity by activating a particular set of antennas at a time instead of all. Thus a MIMO antenna integrated with a lens, transmitarray, or reflectarray (Beam-Switching) can be a better alternative to the conventional beamforming networks at mm-wave frequencies.

A 3D-printed luneberg lens antenna is used in [3] to design a multi-beam antenna at mm-wave frequencies. The antenna uses multiple standard gain horns as feed elements to generate the multiple beams. The use of horn antennas and the 3D Luneberg lens makes the design bulky and difficult to handle. A 1-D beam-switching is achieved in [6] by using a 3-element stacked patch as a spatial excitation to the metasurface lens. The antenna operates from 27.5-32 GHz with a gain of 20.2dBi and a beam scanning of $\pm 15°$. The antenna provides the beam-switching capability only in one direction and can not be used for 2-D beamforming. A lens antenna beam-switching system at 28 GHz for static and mobile usage is reported in [23]. The beam-switching is implemented by utilizing a 1×4 and 4×4 patch MIMO antenna as a feed source. A beam-switching spherical lens operating at E-band (71-76 GHz) is presented in [24]. The spherical lens is fed by a 1×16 linear array based on SP4T switches and a Vivaldi antenna. The beam-switching antenna gives a peak gain of 21.8dBi with a scan loss of 1.3dB for a beam coverage of $\pm 40°$. An E-band integrated lens antenna fed by a 64-element patch MIMO antenna is reported in [25]. The antenna can switch the beam in $\pm 4°$ x $\pm 17°$. Although the designs in [23], [24], and [25] can provide the beam-switching in 2 dimensions, the dielectric lens antenna used in all the methods is difficult to fabricate and handle owing to its curved geometry. A 1-D beam-steering metasurface-based lens antenna working in the frequency range of 1.63-2.24 GHz is reported in [26]. The lens can switch the beam in one principal plane and lacks the beamforming capability in another plane. A liquid crystal-based metasurface reflectarray operating at 108 GHz is presented in [28]. The reflectarray is designed for beamforming and beam splitting
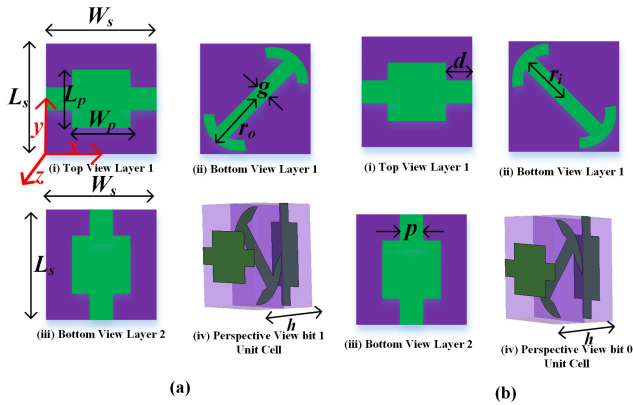
FIGURE 3. Unit cell designs of the proposed 1-bit, two dimensional beam-switching transmitarray antenna (a) Bit-0 (b) Bit-1 with $W_S = L_S = 2.4$ mm $W_P = 1.5$ mm, $L_P = 1.2$ mm, $p = 0.4$ mm, $d = 0.45$ mm, $W_P = L_S = 2.4$ mm, $h = 1.52$ mm, $g = 1.5$ mm, $r_o = 1.15$ mm, $r_i = 0.85$ mm.

with a beam scan coverage of $\pm40°$ in the azimuth and elevation planes. A one-dimensional beam-switching trans-mitarray operating at 30.5 GHz is reported in [29]. The planar transmitarray can switch the beam in one plane while lacking the switching in the orthogonal plane. A 3-layer metasurface lens for two-dimensional coverage operating in a sub-6 GHz band utilizing an 8×8 stacked patch MIMO antenna is presented in [30]. The lens antenna provides a means to steer the beam in both theta and phi directions.

In this paper, a two-dimensional switchable beam trans-mitarray with the phase approximation of 0 and π is pre-sented. The transmitarray's elements have an insertion loss better than 1.5 dB in the frequency range of 24-40 GHz. The polarization rotating phase shift elements change the polarization of the incident linearly polarized y-directed wave into the transmitted linearly polarized x-directed wave. The transmitarray is illuminated by a printed 3×3, 9-element Yagi antenna. The antenna operates over a 26.3-29.3 GHz frequency range, thus giving 10.8 % impedance bandwidth. The antenna has a maximum gain of 19.7 dBi with a switching loss of 1.6 dB. The different beams have a 3-dB beamwidth ranging from 9.8-11.2°. The offset antennas along both x and y-directions give a radiation beam directed along $\pm15°$, thus providing a radiation coverage cone of 30°. The antenna can be deployed in any vehicle for reliable communication with different networks. To overcome the penetration losses in public transport vehicles at mm-wave frequencies, the antenna can be used inside vehicles as a repeater antenna for hassle-free communication.

The key contributions of the proposed work are as follows

1) **Two Dimensional coverage**: The proposed design pro-vides the two-dimensional coverage, i.e., the switch-able beam transmitarray provides the offset radiation beams in both theta and phi-directions. In comparison to the designs reported in [6], [24], [26], and [29], which provide a 1-D radiation coverage, the proposed design generates a radiation coverage cone of 30°.

2) **Wideband Operation**: The phase shift elements of the design provide a low insertion loss of around 1.5 dB in the frequency range of 24-40 GHz, and also, the bit-0 and bit-1 phase shift elements have a phase difference of π in the mentioned frequency band, which confirms the wideband characteristics of the proposed design. However, the operational bandwidth of the antenna is limited by the bandwidth of the feed elements. The feed elements operate in 26.3-29.3 GHz, thus providing a fractional bandwidth of 10.8 %. The wideband standard gain horn antenna can illuminate the proposed transmitarray panel for single beam wideband operation.

3) **Compact Design**: The proposed design is compact in terms of the thickness of the panel, the number of substrate layers, and the focus-to-dimension ratio. The design has a small panel thickness in comparison to the methods reported in [24], [29], and [30]. The f/d ratio of the transmitarray antenna is also small in comparison to [28]. In addition to this, the design also utilizes only two substrate layers. Furthermore, with respect to the designs reported in [6], [24], and [29], which use the air-spacers to hold the substrate layers together, the substrate layers of the proposed design are held together using Teflon screws.

4) **Planar Geometry**: In comparison to the designs pre-sented in [24], [25], and [26], which use the spherically curved geometry lens, the proposed design utilizes a planar geometry transmitarray panel which makes our proposed design easy to handle and fabricate.

5) **Scalable to Massive MIMO applications**: The trans-mitarray panel size of the proposed design can be increased to accommodate more of the feed antennas for applications in the millimetre-wave massive MIMO systems.

6) **Energy Efficient alternative to beamforming**: The proposed design can be an energy-efficient alterna-tive to beamforming networks at millimetre-wave fre-quencies. The beamforming networks require active phase shift circuitry for beam-steering. The proposed design uses a passive phase shift transmitarray panel for beam-steering, which eliminates the use of the active circuitry.

The article's organization is as follows. Section II explains the concept of transmitarray. Section III presents the design of phase shift elements. The feeding array design is presented in section IV. Section V describes the transmitarray design, followed by fabrication and measurement in section VI. Sec-tion VII concludes the paper.

II. CONCEPT OF TRANSMITARRAY ANTENNA

The transmitarray antenna comprises a feed antenna and a thin transmitting panel (Fig. 2). The transmitting panel con-sists of phase shift elements arranged according to the phase distribution. The transmission coefficients of the individual elements are designed such that the incident spherical wave,
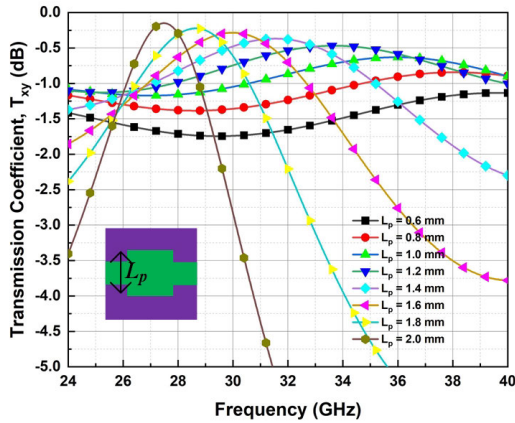
FIGURE 4. Variation in transmission coefficient magnitude with the change in geometrical values of L_p for both bit-0 and bit-1 phase shifting elements.
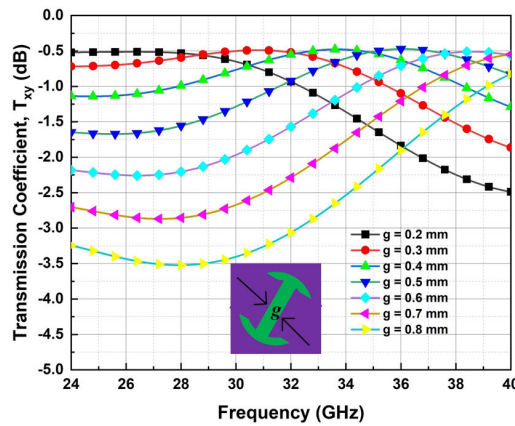

FIGURE 5. Variation in transmission coefficient magnitude with the change in geometrical values of g for both bit-0 and bit-1 phase shifting elements.

FIGURE 6. Simulated transmission coefficient phase of the proposed bit-0 phase shift element for the design of 1-bit two-dimensional beam-switching transmitarray with a variation of L_p.

FIGURE 7. Simulated transmission coefficient phase of the proposed bit-1 phase shift element for the design of 1-bit two-dimensional beam-switching transmitarray with a variation of L_p.

after transmitting through the transmitarray surface, gets transformed into the plane wave collimated in a particular direction. The feed antenna is located at the focal point of the transmitting surface.

The transmitting surface of Fig. 2 is placed in the xy plane with the coordinates of each point on the transmitting surface as $(x_i, y_i, 0)$. Let us assume that the feed antenna is located at some distance d_i from the surface having coordinates (x_f, y_f, z_f). Equation (1) gives the phase of the incident wave

$$\varphi_{in}(x_i, y_i) = k_0 d_i \qquad (1)$$

where $d_i = \sqrt{(x_i - x_f)^2 + (y_i - y_f)^2 + z_f^2}$

To point the beam in a fixed direction (θ_0, ϕ_0), the panel has to introduce the following phase delay (2)

$$\varphi_{surface}(x_i, y_i) = k_0 [d_i - \sin\theta_0 (x_i \cos\varphi_0 + y_i \sin\varphi_0)] \quad (2)$$

Equation (2) gives the continuous phase variation along the surface and will require infinite unit cells to replicate the phase distribution. The phase distribution along the panel can
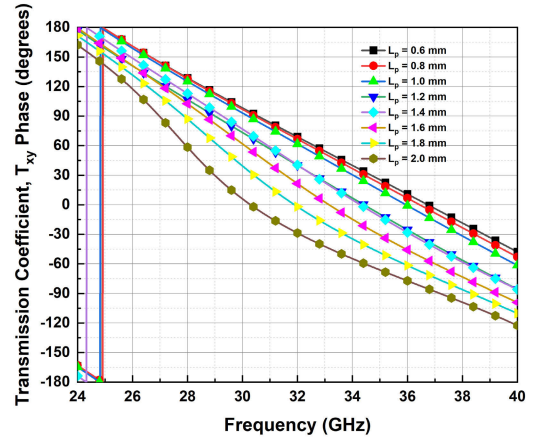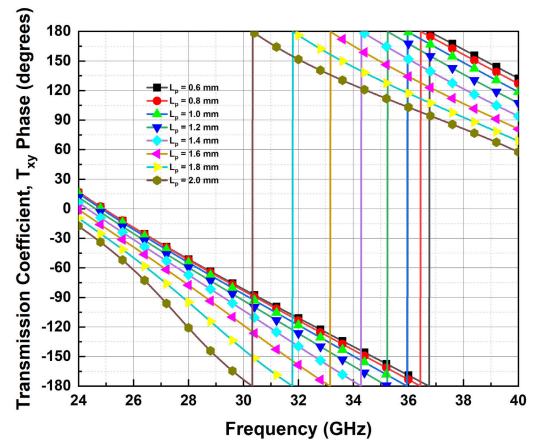
be approximated to various levels to implement a more practical quantized phase distribution. The phase can be quantized into two levels as per the below condition to implement the 1-bit quantized distribution.

$$\begin{cases} \Phi_{surface} \le 90° \text{ or } \Phi_{surface} > 270° \to \Phi_{quant.} = 0° \\ 270° \ge \Phi_{surface} > 90° \to \Phi_{quant.} = 180°. \end{cases}$$

Thus two phase shift elements having a phase difference of 180° are required to implement a 1-bit phase quantized distribution. Similarly, a 2-bit phase quantized distribution can be implemented by four phase shift elements having a progressive 90° phase difference.

$$\begin{cases} 0° \ge \Phi_{surface} > 90° \to \Phi_{quant.} = 0° \\ 90° \ge \Phi_{surface} > 180° \to \Phi_{quant.} = 90° \\ 180° \ge \Phi_{surface} > 270° \to \Phi_{quant.} = 180° \\ 270° \ge \Phi_{surface} > 360° \to \Phi_{quant.} = 270°. \end{cases}$$
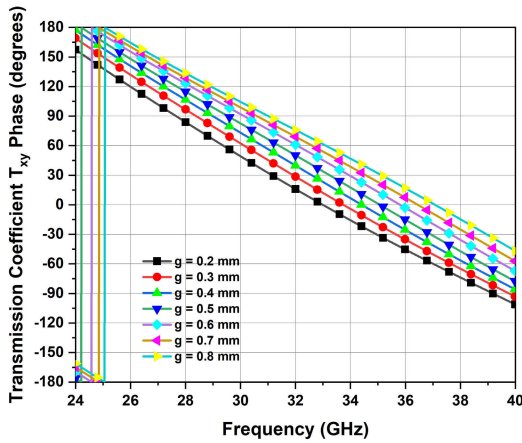
FIGURE 8. Simulated transmission coefficient phase of the proposed bit-0 phase shift element for the design of 1-bit two-dimensional beam-switching transmitarray with a variation of *g*.
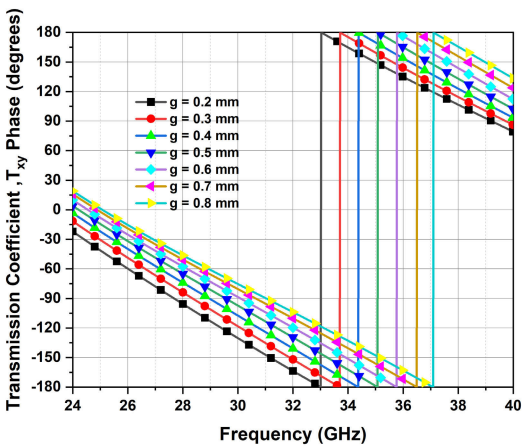

FIGURE 9. Simulated transmission coefficient phase of the proposed bit-1 phase shift element for the design of 1-bit two-dimensional beam-switching transmitarray with a variation of *g*.

III. TRANSMITARRAY PHASE SHIFT ELEMENT DESIGN AND SIMULATION

Fig. 3 presents the bit-1 and bit-0 phase shift elements of the proposed transmitarray antenna. The elements consist of two dielectric layers and three metallic layers. Rogers Diclad-880 with thickness, $t = 0.762\ mm$, $\epsilon_r = 2.2$ and $tan\delta = 0.0009$ is used as a substrate for the design of the phase-shifting element.

The top dielectric layer is printed on both sides with the metallic layers (top and middle layer), while the bottom dielectric layer has only one metallic layer (bottom layer). The two substrate layers are put together by Teflon screws. The top and bottom metallic layers are orthogonally rotated metallic cross structures, while the middle metallic layer is $\pm 45°$ rotated end-loaded dipole structure. The phase shift element is simulated using a CST microwave studio's frequency domain solver by applying the unit cell boundary conditions. The $\pm 45°$ rotation in the end-loaded dipole structure gives rise to two distinct phase elements having a phase difference of 180°. The middle layer not only helps in getting the distinct
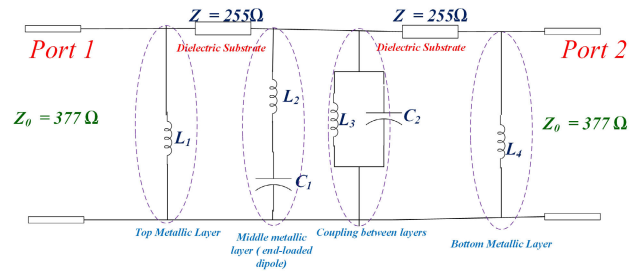

FIGURE 10. Equivalent circuit model of the proposed unit cell with $L_1 = 2$ nH, $L_2 = 14$ nH, $L_3 = 4.7$ nH, $L_4 = 12.4$ nH, $C_1 = 0.006$ pF and $C_2 = 0.003$ pF.
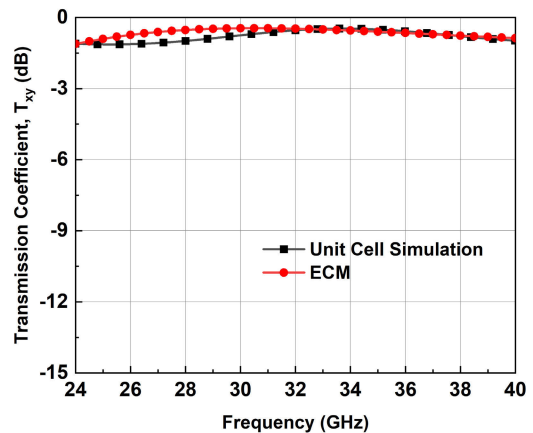

FIGURE 11. Transmission coefficient magnitude of the proposed unit cell in full-wave simulation and equivalent circuit model.

phase shift elements but also helps in improving the transmission coefficient magnitude and rotating the polarization of the incident wave, i.e., the y-polarized wave at the input gets converted to the x-polarized wave at the output.

In order to get the wideband transmission response, a parametric simulation analysis is done. It is found that the transmission bandwidth of the proposed phase shift elements depends mainly on two parameters, i.e, the length of the top and bottom metallic patches (L_p) and the width of the 45° rotated end-loaded dipole (*g*). Fig. 4 shows the transmission coefficient magnitude response (same for both bits) of the phase shift elements for varying lengths of the top and bottom metallic patches (L_p), keeping all other geometrical parameters constant. It is found that by increasing the length of the patches from 0.6 mm to 1.2 mm, an improvement in transmission coefficient magnitude is seen in the 24-40 GHz frequency band. Further increasing the length of the patches, a decrease in transmission bandwidth is seen. Thus, the length of the patches is chosen to be 1.2 mm.

Another parameter which determines the transmission bandwidth of the phase shift elements is *g* (width of the 45° rotated end-loaded dipole). The parametric study shown in Fig. 5 is done to choose the width of the end-loaded dipole. It is found that by increasing the width from 0.2 mm to 0.4 mm, an increase in transmission bandwidth through the
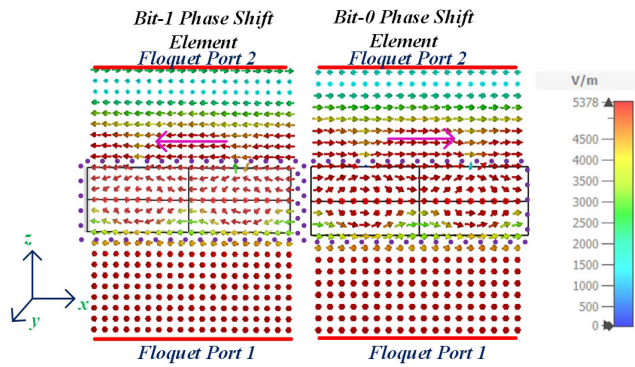
FIGURE 12. Simulated electric field flow from floquet port 1 to 2 in xz-plane of the proposed phase shift elements.
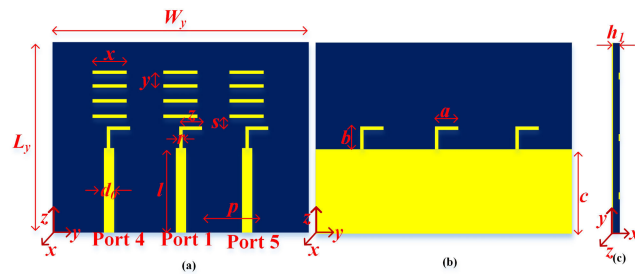

FIGURE 13. 3-port Yagi array antenna used to feed the proposed two-dimensional beam-switching transmitarray (a & b) Side Views (c) Top View with $W_y = 30$ mm, $L_y = 21.7$ mm, $l = 9.1$ mm, $d_0 = 0.78$ mm, $r = 0.4$ mm, $x = 3.4$ mm, $y = 1.6$ mm, $a = z = 2.55$ mm, $b = 2.28$ mm, $c = 10.45$ mm, $s = 1.4$ mm.

phase shift elements is seen. The further increase in the width of the end-loaded dipole degrades the transmission coefficient through the phase shift elements. When the length L_p of the top and bottom metallic patches is increased, the effective surface area of the metal strip also increases. The increase in the length L_p of the metal patches also leads to an increase in the inductance, which results in a higher impedance of the unit cell. This increased impedance reduces the reflection coefficient magnitude and, in turn, increases the transmission coefficient magnitude. The same argument holds good for the increase in the width g of the end-loaded dipole. The increase in the width of the metallic strips increases the transmission up to a certain level; after that, the further increase in the width leads to a shift in the resonance frequency.

The equivalent circuit model shown in Fig. 10 can be used to validate the above argument. The top metallic layer of the unit cell can be modelled as a lumped inductor in shunt configuration, which arises because of the metallic strip. The inter-unit cell capacitance has a very weak effect on the overall transmission coefficient and can be ignored. Similarly, the bottom metallic layer, which is orthogonal to the top metallic layer, can also be modelled as a shunt inductor. The middle layer (45° end-loaded dipole) can be modelled by an inductor and capacitor, which are connected in series. The substrate is modelled as a transmission line having an impedance of
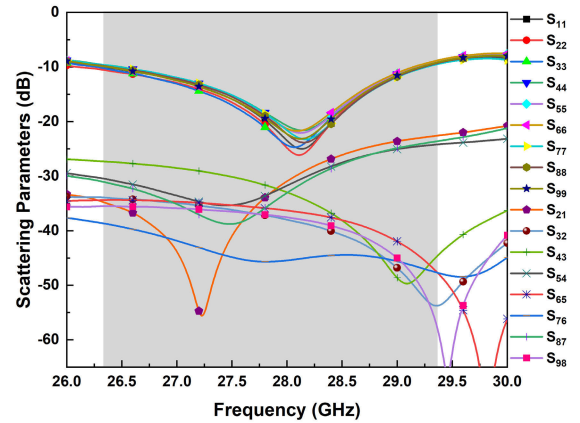

FIGURE 14. Simulated S-parameters of the 9 port Yagi MIMO antenna used as a feeding array to the transmitarray panel.

TABLE 1. Parametric variation of the aperture efficiency, gain and sll with the f/d ratio.

f/d	TA Gain (dBi)	SLL (dB)	E-plane HPBW (°)	H-plane HPBW (°)	Aperture Efficiency (%)
0.33	17.7	12.8	12.4	10.8	14.9
0.42	18.8	15.3	10.4	9.7	19.2
0.50	19.7	18.1	9.5	9	23.6
0.58	18.3	15.7	9.1	8.8	17.1
0.67	17	14.2	8.8	8.8	12.6

$Z_0/\sqrt{\epsilon_r}$ (255 Ω) with a length of transmission line equal to the height of the substrate (0.762 mm). In addition to this, the coupling between the layers of the unit cell can be modelled by the parallel combination of L_3 and C_2. Fig. 11 shows the transmission coefficient of the equivalent circuit model and the unit cell. It is seen from Fig. 11 that the equivalent circuit response is almost similar to the full wave EM response of the unit cell.

Any change in the lengths L_p or g will lead to the change in L_1, L_2, L_3, L_4, C_1 and C_2, which will result in the change in input impedance and will change transmission coefficient of the unit cell.

There is no effect on the phase difference between the two elements by varying L_p and g as the phase difference depends on the orientation of the end-loaded dipole. The variation of the phase of the elements with varying L_p is shown in Figs. 6 and 7, which depicts that the phase of the two elements changes with the change in L_p, but the phase difference between the bit-0 and bit-1 elements remains constant (180°). The parametric study is done to see the effect of varying the geometrical parameter g on the phase difference of elements. From Figs. 8 and 9, it can be concluded that the variation of g has an almost negligible effect on the phase difference. The proposed phase shift elements have a maximum insertion loss of approximately 1.5 dB, and the phase difference between the bit-0 and bit-1 elements is 180° in the 24-40 GHz frequency band.
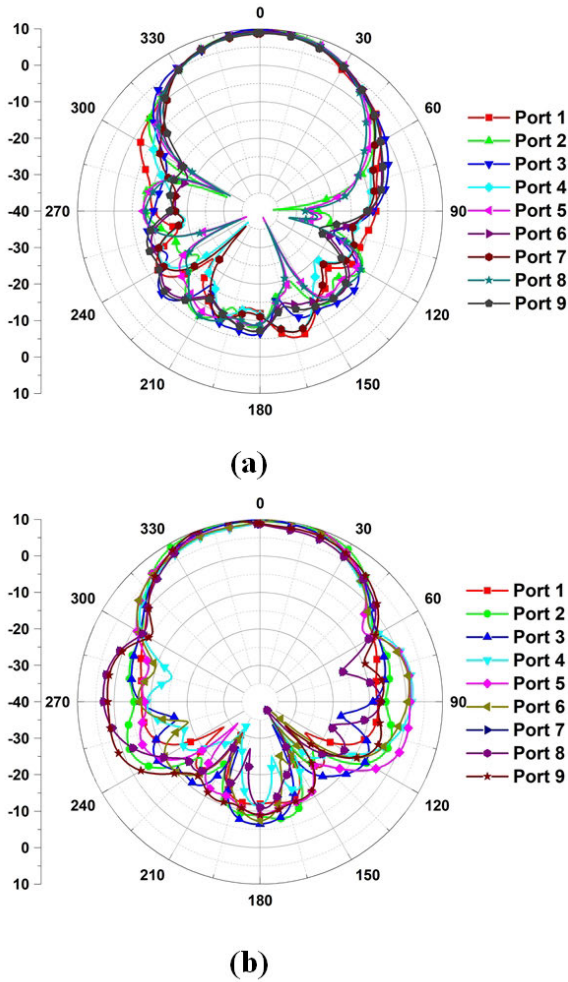
(a)

(b)

FIGURE 15. Simulated Co-polar radiation patterns of the MIMO Yagi feed source in (a) xz-plane (b) yz-plane.

TABLE 2. Parametric variation of the aperture efficiency with the number of directors for a fixed aperture area and f/d of 0.5.

Antenna Type	TA Gain (dBi)	Aperture Efficiency (%)
MDA	17	12.6
MDA with 1 director	18	16
MDA with 2 directors	19	20.1
MDA with 3 directors	19.4	22
MDA with 4 director	19.7	23.6

The instantaneous electric field flow from floquet port 1 to 2 of the phase shift elements is shown in Fig. 12. It can be observed from Fig. 12 that the incident y-polarized electric field from floquet port-1 gets converted to the x-polarized field after transmission through both the phase shift elements. The direction of the transmitted electric field through the elements is opposite to each other, which validates that the phase difference between the transmission coefficients of both the elements is 180°. Thus the proposed phase delay elements are suitable candidates for designing a 1-bit transmitarray.
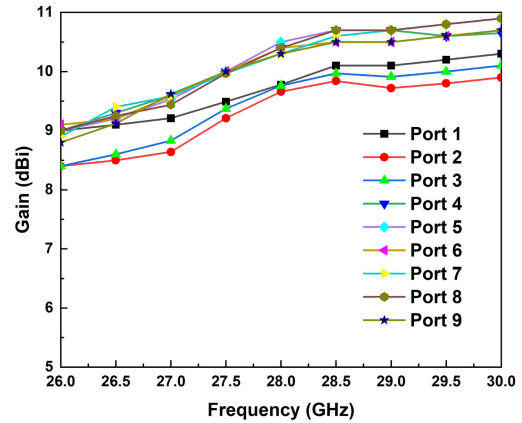

FIGURE 16. Simulated gain of the 9 port Yagi MIMO antenna used as a feeding array to the transmitarray panel.
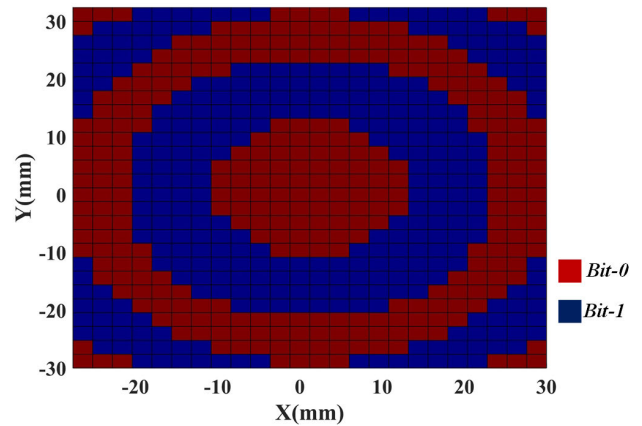

FIGURE 17. Quantized phase distribution of the proposed two-dimensional switchable beam transmitarray for focal distance, $f = 30mm$ at 28 GHz.

IV. FEEDING ARRAY DESIGN AND SIMULATION

A printed microstrip dipole antenna (MDA) operating in the range of 26.3-29.3 GHz is designed. The four directors are added to the MDA to arrive at the design of a microstrip-printed Yagi antenna. The number of directors used in the feed Yagi antenna affects its 3dB beamwidth and gain. The 3 Yagi antennas, each having three individual elements (Fig. 13), are designed in a 3 × 3 (9-antenna elements) configuration to feed the transmitarray panel. The inter-element spacing in the feed array is 10 mm. Fig. 13 shows the side views and the top view of the proposed 3-port Yagi array antenna. The other two 3-port Yagi antennas are placed at the offset of $\pm10mm$ along the x-axis. The Yagi antenna is designed on a Rogers Diclad-880 substrate with thickness $h_1 = 0.254\ mm$, $\epsilon_r = 2.2$ and $tan\delta = 0.0009$.

Fig. 14 shows the S-parameters of the 9-port Yagi array antenna. The antennas operate in 26.3−29.3 GHz with a fractional bandwidth of 10.8%. The array antenna elements also have low mutual coupling (20 dB) between different antenna ports in the working frequency (26.3−29.3 GHz).
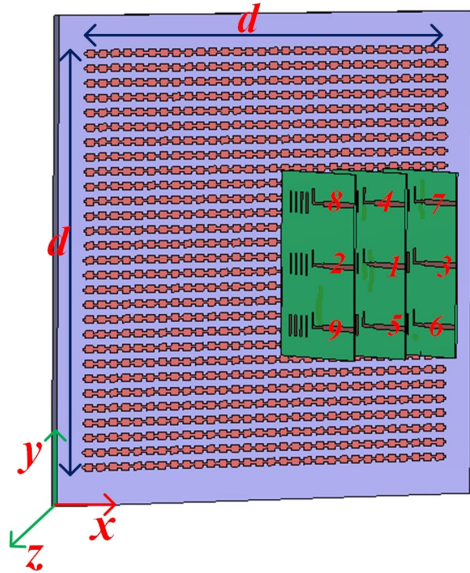
FIGURE 18. Perspective view of the proposed two-dimensional beamforming transmitarray antenna with $d = 60mm$ (The numbers on the antenna elements denote the port numbers).
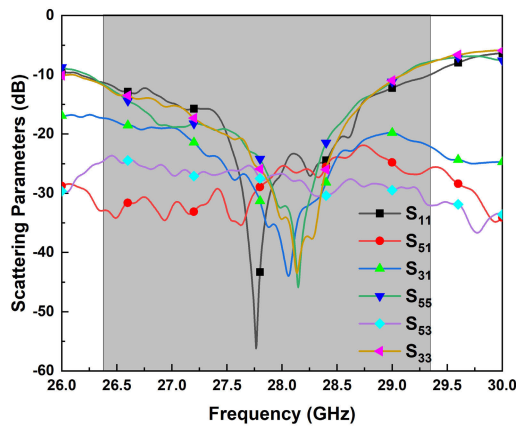

FIGURE 19. Simulated S-parameters of the proposed two-dimensional beam-switching transmitarray.

FIGURE 20. Simulated 3-D Radiation patterns of the proposed two-dimensional beam-switching transmitarray at 28 GHz (a) port 1 (b) port 5 (c) port 3 (d) port 7.
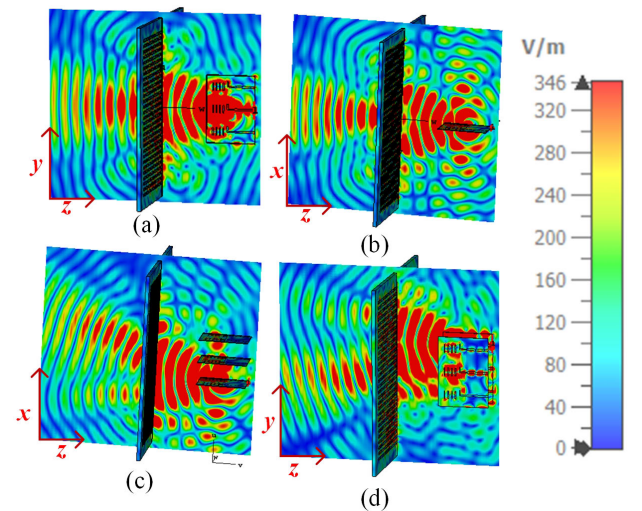
FIGURE 21. Electric field focussing of the proposed two-dimensional beam-switching transmitarray (a and b) port 1 (c) port 2 (d) port 4.

The radiation pattern of the 9-port MIMO antenna at 28 GHz in both the principle planes is presented in Fig. 15. The different antenna elements have an approximately equal gain of 9.5dBi at 28 GHz with a 3 dB beamwidth of around 60° in both xz and yz-planes. Fig. 16 shows the gain of each antenna element used to feed the transmitarray panel. The radiation in the offset antennas mitigates with the radiation of ports 1, 2 and 3, which slightly decreases the gain of these antennas. The proposed feed antenna is less complex in terms of geometry and is less prone to fabrication and measurement errors.

V. TRANSMITARRAY DESIGN AND ITS INTEGRATION WITH THE 9 PORT YAGI ARRAY ANTENNA

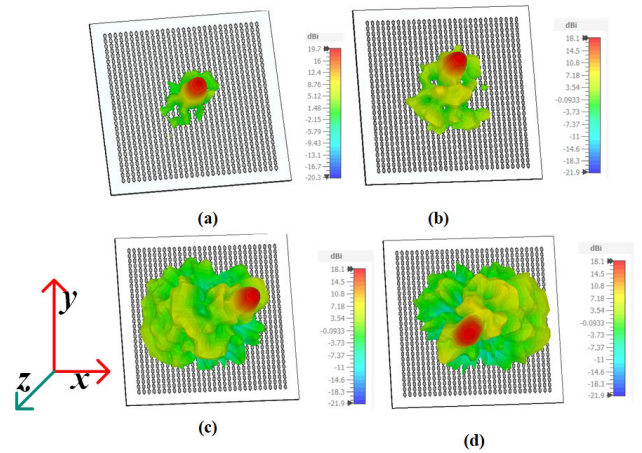In a transmitarray, the incident spherical waves from the excitation element transmit through the panel to produce the directive beam at the output. As already discussed, the direction of the outgoing beam is dependent on the position of the feed and the phase distribution along the surface of the transmitarray. In order to concentrate the beam in the broadside direction with the feed positions as (0,0,30mm), the approximated distribution of the proposed transmitarray taking 25 × 25 (60mm x 60mm) array of the phase shift elements at 28 GHz is shown in Fig. 17.

The phase shift elements are arranged according to the phase distribution in Fig. 17 to design a transmitarray panel. The transmitarray panel is fed by a 3 × 3, 9 port Yagi array antenna to arrive at the design of a two-dimensional switchable beam transmitarray. The integrated antenna system is simulated in the time domain solver of the CST Microwave studio. Fig. 18 shows the two-dimensional beam-switching transmitarray antenna. The simulated S-parameters of the transmitarray antenna are shown in Fig. 19. The results
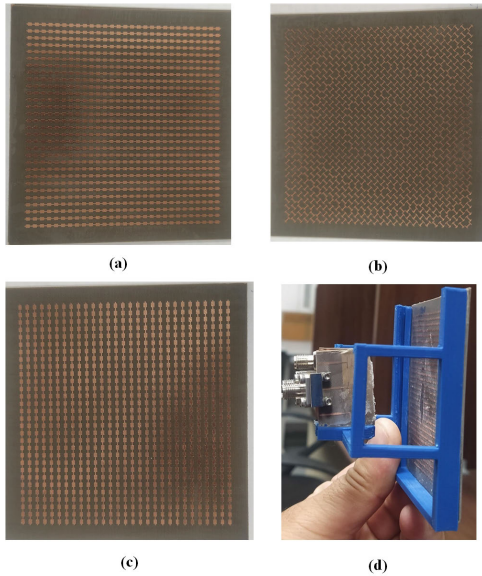
FIGURE 22. Prototype of the proposed two-dimensional beam-switching transmitarray (a) Top view of Layer 1 (b) Bottom view of Layer 1 (c) Bottom view of Layer 2 (d) full fabricated prototype.
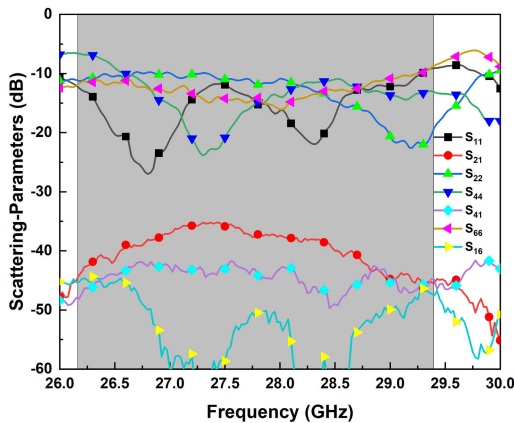

FIGURE 23. Measured S-Parameters of the proposed two dimension beam-switching transmitarray.

show that the antenna operates in the 26.3-29.3 GHz frequency band with isolation between ports greater than 20 dB at 28 GHz. The simulated 3-D radiation patterns of the transmitarray are shown in Fig. 20. The 3-D radiation patterns show that the excitation of port 1 gives a radiation beam in the broadside direction with a gain of 19.7 dBi without any tilt, whereas the excitation of the ports 2 and 3 give the radiation beam in the broadside direction with a tilt in +x-axis and -x-axis and a scan loss of 1.6 dB, respectively. Similarly, ports 4 and 5 excitations give the radiation beams tilted in the -y-axis and +y-axis, respectively. The excitation of ports 6, 7, 8 and 9 give radiation beams tilted in x and y-axes. For brevity, only the 3-D radiation pattern of ports 1, 3, 5 and 7 are shown in Fig. 20.

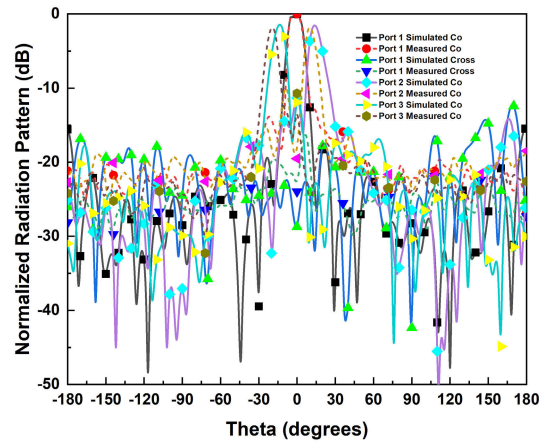One of the important design considerations of the transmitarray is the aperture efficiency which is the ratio of the

FIGURE 24. Simulated and measured radiation patterns of the proposed two-dimensional switchable beam transmitarray at 27 GHz in xz-plane.
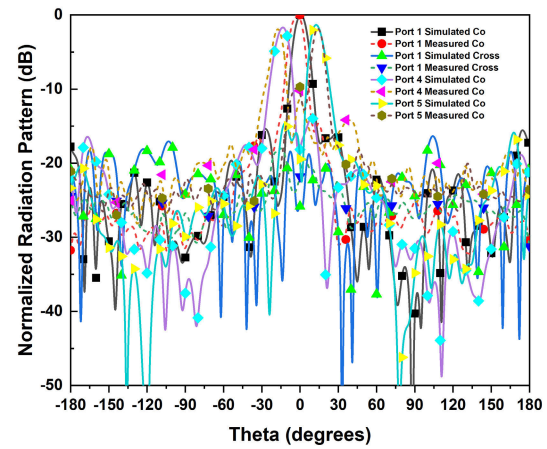

FIGURE 25. Simulated and measured radiation patterns of the proposed two-dimensional switchable beam transmitarray at 27 GHz in yz-plane.

effective radiating area to the physical area of the aperture. The aperture efficiency of the antenna is calculated by the following equation given in [31]

$$e_a = \frac{10^{\left(\frac{G_{dB}}{10}\right)}\lambda^2}{4\pi A_p} \qquad (3)$$

where G_{dB} is the gain of transmitarray in dBi, λ is the operating wavelength and A_p is the physical aperture area of the transmitarray.

The aperture efficiency of the transmitarray mainly depends on the physical aperture area and gain. The aperture efficiency is 23.6% at 28 GHz for the proposed transmitarray. A parametric study is done to find the optimal focal point, where the antenna gain and aperture efficiency is maximum and the side-lobe level is minimum. Table 1 shows that for an f/d ratio of 0.5, the gain and aperture efficiency is maximum, and the side-lobe level (SLL) is minimum.

Since the feed antenna used in the proposed design is the Yagi antenna, whose gain and the 3 dB beamwidth can be controlled by the use of a number of directors, a parametric study is done to enhance the aperture efficiency of the
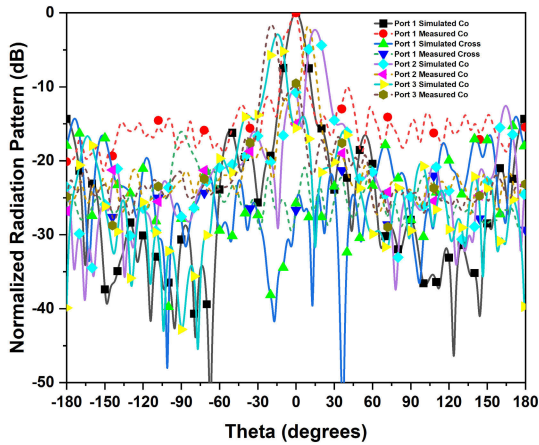
FIGURE 26. Simulated and measured radiation patterns of the proposed two-dimensional switchable beam transmitarray at 29 GHz in xz-plane.
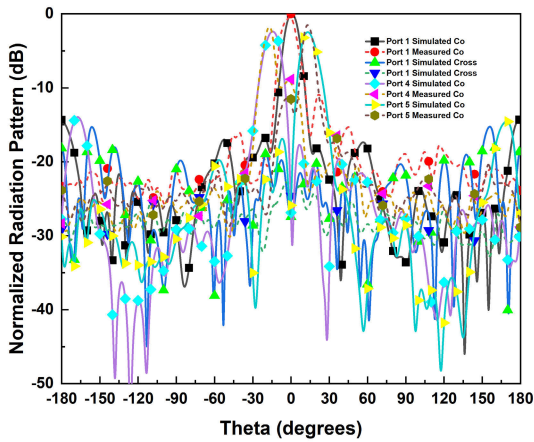

FIGURE 27. Simulated and measured radiation patterns of the proposed two-dimensional switchable beam transmitarray at 29 GHz in yz-plane.

FIGURE 28. Measured gain of the proposed two dimensions beam-switching transmitarray for different antenna ports in the direction of maximum radiation.

TABLE 3. Summary of the performance of the different antenna ports.

Port No.	Gain (dBi)	Beam Direction (phi,theta)	3-dB Beamwidth(°)
1	19.7	(0°,0°)	9.8
2	18.1	(90°,-15°)	11
3	18.1	(90°,15°)	11
4	18.1	(0°,-15°)	11
5	18.1	(0°,15°)	11
6	18.1	(-45°,20°)	11.2
7	18.1	(45°,-20°)	11.2
8	18.1	(135°,-20°)	11.2
9	18.1	(-135°,20°)	11.2

proposed design. The parametric study is done for a fixed area of the aperture (60 mm x 60 mm) at a frequency of 28 GHz with a focus-to-dimension ratio (f/d) of 0.5, as shown in Table 2. As the number of directors in the feed antenna is increased (which effectively reduces the 3dB beamwidth and enhances the gain), the aperture efficiency also gets increased. An aperture efficiency of 23.6% is obtained for the proposed design when the number of directors used is four.

The summary of the performance of the different ports of the antenna is shown in Table 3. The performance parameters of the 9-port beam-switching antenna show its capability to switch the beams in both the principal planes with high gain and low scan loss. Fig. 21 shows the electric field focusing of the proposed transmitarray when ports 1, 2, and 4 are excited. The focus of the beam-switching transmitarray antenna shows that the panel can steer the radiation in different directions.

VI. FABRICATION AND MEASUREMENT

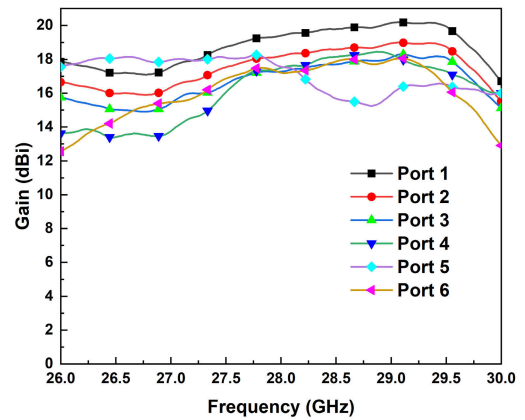The proposed two-dimensional switchable beam transmitarray is fabricated as shown in Fig. 22. As the antenna systems at mm-wave frequencies have less tolerance to any change in dimension, it is ensured that the exact dimensions are printed on the substrate as a small variation in the fabrication dimension may lead to an undesired response of the antenna system. The Teflon-based screws are used to hold the two substrate layers together. A 3D printed stand is fabricated to hold the feed antennas and the transmitarray panel to ensure that the feed antennas are at the exact position. A 2.92 mm Hirose connector (HK-LR-SR2(12)) is used to feed each element. The Anechoic chamber at IIT Jammu is used to experimentally verify the performance parameters using a vector network analyzer (N5224B). The measured S-parameters of the proposed transmitarray are shown in Fig. 23. The measured S-parameter results show an operating impedance bandwidth of 10.8% (26.3-29.3GHz) with isolation between different ports better than 20 dB. The slight difference between the simulated and measurement results is because of fabrication and measurement errors. The 2D radiation patterns of the proposed two-dimensional switchable beam transmitarray have been measured at 27 GHz, 27.5 GHz, 28 GHz, 28.5 GHz, 29 GHz, and 29.5 GHz in xz and yz-planes.

Fig. 24-27 shows the radiation patterns of the proposed switchable beam transmitarray in the xz and yz planes at 27 and 29 GHz. The radiation pattern results show a 3-dB beamwidth of the antenna ranging from 9.8 to 11.2° in different antenna ports. The offset antennas in both x and y directions give a tilted radiation beam whose direction is

TABLE 4. State of the art comparison of the switchable beam transmitarray with the reported transmitarrays.

Ref.	f(GHz)	Layers	Thickness (λ_0)	f/d	Surface Size (λ_0^2)	Gain (dBi)	BS cap.	SLL	MIMO type
[6]	29.75	2	0.12	0.2	5.55 x 5.55	20.1	1-D	10 dB	3-Element ACPA
[8]	30	2	0.113	0.52	10 x 10	24.2	NA	15 dB	NA
[9]	77	4	0.1	NA	NA	NA	NA	NA	NA
[24]	1.95	5	0.42	0.14	2.6 x 2.6	10-13.5	1-D	15 dB	1 x 4 cross dipole with metasurface loading
[25]	73.5	Dielectric lens	NA	NA	NA	21.8	1-D	NA	1 x 16 Vivaldi Array
[29]	30.5	2	0.304	0.49	6.2 x 6.2	19.3	1-D	15 dB	3-element patch
[30]	5.8	3	0.46	0.56	10 x 10	22.4	two Dimension	20 dB	8 x 8 patch array
[32]	6	3	0.8	1	5.4 x 5.4	20.1	15 dB	NA	NA
[This Work]	27.8	2	0.147	0.5	5.6 x 5.6	19.7 dBi	2-D	12 dB	3 x 3 Yagi Array

shown in table 3. The proposed transmitarray provides a radiation cone of 30°. Fig. 28 shows the measured gains of the different parts of the proposed switchable beam transmitarray. The measured peak gain of approximately 19.7 dB is obtained for port 1, with a switching loss in the rest of the ports.

The comparative study of the proposed antenna with the literature is shown in table 4. The proposed transmitarray can switch the radiation beam in two dimensions, i.e., both theta and phi directions, utilizing a two-dimensional 9-port Yagi-array feed. The proposed design uses fewer substrate layers than [24] and [30]. The thickness of the transmitarray panel is also smaller in comparison to [6], [24], [26], [29], and [30]. The proposed design is compact, having an f/d ratio of 0.5, smaller than [30].

VII. CONCLUSION

This paper presents a compact, two-dimensional beam-switching transmitarray antenna for millimetre-wave (26.3-29.3 GHz) applications having an impedance bandwidth of 10.8%. The transmitarray panel utilizes a 9-port Yagi array antenna as a feed to implement the beam-switching. The MIMO antenna elements have isolation between different ports better than 20 dB in the frequency band of $26.3 - 29.3$ GHz. The transmitarray has a peak gain of 19.7 dBi in the central feeding element with a scan loss of 1.6 dB in the offset antennas. The radiation beams in different directions are highly directive, with a 3 dB beamwidth ranging from $9.8 - 11.2$ °. The two-dimensional angular coverage, which is determined by the radiation cone, is 30° for the proposed antenna. The proposed transmitarray is compact, having a small f/d ratio of 0.5. Due to the compactness of the design, a large number of these antennas can be accommodated in the base station to direct a beam to a specific user. The proposed antenna can be installed in a public transport vehicle as a repeater antenna to direct the beam to different users travelling inside a vehicle. The antenna can also be used in mm-wave base stations to direct the electromagnetic wave to specific users. Furthermore, the transmitarray panel size can be increased to accommodate more antennas, i.e., the proposed design is scalable and can be a good candidate

for the realization of massive MIMO antenna systems. A Ka-band horn antenna can be used to feed the transmitarray panel for single beam wideband operation. In addition to this, the phase quantization levels in the transmitarray panel can be increased to have a high phase resolution, resulting in higher gain and higher aperture efficiency. Furthermore, the 1:9 microwave switch can be used in conjunction with the feed antenna to efficiently implement beam-switching in practical applications. A programmable microcontroller unit can be used with the 1:9 microwave switch to make the beam directions programmable, i.e. depending upon the required beam direction, a fixed antenna can be turned on to get the desired direction. The proposed design is energy efficient as it does not use the phase shifters to steer the beam in a particular direction.

REFERENCES

[1] A. Osseiran, F. Boccardi, V. Braun, K. Kusume, P. Marsch, M. Maternia, O. Queseth, M. Schellmann, H. Schotten, H. Taoka, H. Tullberg, M. A. Uusitalo, B. Timus, and M. Fallgren, "Scenarios for 5G mobile and wireless communications: The vision of the METIS project," *IEEE Commun. Mag.*, vol. 52, no. 5, pp. 26–35, May 2014.

[2] *LTE-Advanced Pro Pushing LTE Capabilities Towards 5G*, Nokia Netw., Espoo, Finland, Dec. 2015. Accessed: Oct. 15, 2017. [Online]. Available: https://resources.ext.nokia.com/asset/200176

[3] Y. Guo, Y. Li, J. Wang, L. Ge, Z. Zhang, M. Chen, Z. Li, B. Ai, and R. He, "A 3D printed nearly isotropic Luneburg lens antenna for millimeter-wave vehicular networks," *IEEE Trans. Veh. Technol.*, vol. 71, no. 2, pp. 1145–1155, Feb. 2022, doi: 10.1109/TVT.2021.3134703.

[4] T. S. Rappaport, S. Sun, R. Mayzus, H. Zhao, Y. Azar, K. Wang, G. N. Wong, J. K. Schulz, M. Samimi, and F. Gutierrez, "Millimeter wave mobile communications for 5G cellular: It will work!" *IEEE Access*, vol. 1, pp. 335–349, 2013, doi: 10.1109/ACCESS.2013.2260813.

[5] K. Gulur Sadananda, M. P. Abegaonkar, and S. K. Koul, "Gain equalized shared-aperture antenna using dual-polarized ZIM for mmWave 5G base stations," *IEEE Antennas Wireless Propag. Lett.*, vol. 18, no. 6, pp. 1100–1104, Jun. 2019, doi: 10.1109/LAWP.2019.2910183.

[6] Z. Wani, M. P. Abegaonkar, and S. K. Koul, "Thin planar metasurface lens for millimeter-wave MIMO applications," *IEEE Trans. Antennas Propag.*, vol. 70, no. 1, pp. 692–696, Jan. 2022, doi: 10.1109/TAP.2021.3098571.

[7] E. B. Lima, S. A. Matos, J. R. Costa, C. A. Fernandes, and N. J. G. Fonseca, "Circular polarization wide-angle beam steering at Ka-band by in-plane translation of a plate lens antenna," *IEEE Trans. Antennas Propag.*, vol. 63, no. 12, pp. 5443–5455, Dec. 2015, doi: 10.1109/TAP.2015.2484419.

[8] L. Di Palma, A. Clemente, L. Dussopt, R. Sauleau, P. Potier, and P. Pouliguen, "Circularly polarized transmitarray with sequential rotation in Ka-band," *IEEE Trans. Antennas Propag.*, vol. 63, no. 11, pp. 5118–5124, Nov. 2015, doi: 10.1109/TAP.2015.2474149.

[9] C. Pfeiffer and A. Grbic, "Millimeter-wave transmitarrays for wavefront and polarization control," *IEEE Trans. Microw. Theory Techn.*, vol. 61, no. 12, pp. 4407–4417, Dec. 2013, doi: 10.1109/TMTT.2013.2287173.

[10] W. Hong, Z. H. Jiang, C. Yu, J. Zhou, P. Chen, Z. Yu, H. Zhang, B. Yang, X. Pang, M. Jiang, Y. Cheng, M. K. T. Al-Nuaimi, Y. Zhang, J. Chen, and S. He, "Multibeam antenna technologies for 5G wireless communications," *IEEE Trans. Antennas Propag.*, vol. 65, no. 12, pp. 6231–6249, Dec. 2017, doi: 10.1109/TAP.2017.2712819.

[11] Y. Zeng and R. Zhang, "Millimeter wave MIMO with lens antenna array: A new path division multiplexing paradigm," *IEEE Trans. Commun.*, vol. 64, no. 4, pp. 1557–1571, Apr. 2016, doi: 10.1109/TCOMM.2016.2533490.

[12] M. Karabacak, H. Arslan, and G. Mumcu, "Lens antenna subarrays in mmWave hybrid MIMO systems," *IEEE Access*, vol. 8, pp. 216634–216644, 2020, doi: 10.1109/ACCESS.2020.3041633.

[13] J.-H. Ou, Z. Chen, S. Fei Bo, Y. Zhang, and X. Yin Zhang, "Compact dual-polarized antenna with low-pass response for marine communication," *IEEE Trans. Veh. Technol.*, vol. 70, no. 3, pp. 2649–2656, Mar. 2021, doi: 10.1109/TVT.2021.3061799.

[14] H. Ozpinar, S. Aksimsek, and N. T. Tokan, "A novel compact, broadband, high gain millimeter-wave antenna for 5G beam steering applications," *IEEE Trans. Veh. Technol.*, vol. 69, no. 3, pp. 2389–2397, Mar. 2020, doi: 10.1109/TVT.2020.2966009.

[15] S. Yu, H. Liu, and L. Li, "Design of near-field focused metasurface for high-efficient wireless power transfer with multifocus characteristics," *IEEE Trans. Ind. Electron.*, vol. 66, no. 5, pp. 3993–4002, May 2019, doi: 10.1109/TIE.2018.2815991.

[16] Y. Zhang, J.-Y. Deng, D. Sun, J.-Y. Yin, and L.-X. Guo, "Compact slow-wave SIW H-plane horn antenna with increased gain for vehicular millimeter wave communication," *IEEE Trans. Veh. Technol.*, vol. 70, no. 7, pp. 7289–7293, Jul. 2021, doi: 10.1109/TVT.2021.3090096.

[17] W. Roh, J.-Y. Seol, J. Park, B. Lee, J. Lee, Y. Kim, J. Cho, K. Cheun, and F. Aryanfar, "Millimeter-wave beamforming as an enabling technology for 5G cellular communications: Theoretical feasibility and prototype results," *IEEE Commun. Mag.*, vol. 52, no. 2, pp. 106–113, Feb. 2014.

[18] J. Jang, M. Chung, S. C. Hwang, Y.-G. Lim, H.-J. Yoon, T. Oh, B.-W. Min, Y. Lee, K. S. Kim, C.-B. Chae, and D. K. Kim, "Smart small cell with hybrid beamforming for 5G: Theoretical feasibility and prototype results," *IEEE Wireless Commun.*, vol. 23, no. 6, pp. 124–131, Dec. 2016.

[19] P. Taghikhani, K. Buisman, and C. Fager, "Hybrid beamforming transmitter modeling for millimeter-wave MIMO applications," *IEEE Trans. Microw. Theory Techn.*, vol. 68, no. 11, pp. 4740–4752, Nov. 2020, doi: 10.1109/TMTT.2020.2995657.

[20] T. Chaloun, L. Boccia, E. Arnieri, M. Fischer, V. Valenta, N. J. G. Fonseca, and C. Waldschmidt, "Electronically steerable antennas for future heterogeneous communication networks: Review and perspectives," *IEEE J. Microw.*, vol. 2, no. 4, pp. 545–581, Oct. 2022, doi: 10.1109/JMW.2022.3202626.

[21] V. G. Ataloglou, M. Chen, M. Kim, and G. V. Eleftheriades, "Microwave Huygens' metasurfaces: Fundamentals and applications," *IEEE J. Microw.*, vol. 1, no. 1, pp. 374–388, Jan. 2021, doi: 10.1109/JMW.2020.3034578.

[22] L. Ren, B. Lu, F. Lu, and Y. Shu, "Modular and scalable millimeter-wave patch array antenna for 5G MIMO and beamforming," in *Proc. 50th Eur. Microw. Conf. (EuMC)*, Jan. 2021, pp. 336–339, doi: 10.23919/EUMC48046.2021.9338130.

[23] Y. J. Cho, G.-Y. Suk, B. Kim, D. K. Kim, and C.-B. Chae, "RF lens-embedded antenna array for mmWave MIMO: Design and performance," *IEEE Commun. Mag.*, vol. 56, no. 7, pp. 42–48, Jul. 2018, doi: 10.1109/MCOM.2018.1701019.

[24] A. E. I. Lamminen, S. K. Karki, A. Karttunen, M. Kaunisto, J. Säily, M. Lahdes, J. Ala-Laurinaho, and V. Viikari, "Beam-switching dual-spherical lens antenna with low scan loss at 71–76 GHz," *IEEE Antennas Wireless Propag. Lett.*, vol. 17, no. 10, pp. 1871–1875, Oct. 2018, doi: 10.1109/LAWP.2018.2868543.

[25] J. Ala-Laurinaho, J. Aurinsalo, A. Karttunen, M. Kaunisto, A. Lamminen, J. Nurmiharju, A. V. Räisänen, J. Säily, and P. Wainio, "2-D beam-steerable integrated lens antenna system for 5G *E*-band access and backhaul," *IEEE Trans. Microw. Theory Techn.*, vol. 64, no. 7, pp. 2244–2255, Jul. 2016, doi: 10.1109/TMTT.2016.2574317.

[26] T. Li and Z. N. Chen, "Compact wideband wide-angle polarization-free metasurface lens antenna array for multibeam base stations," *IEEE Trans. Antennas Propag.*, vol. 68, no. 3, pp. 1378–1388, Mar. 2020, doi: 10.1109/TAP.2019.2938608.

[27] Q. Zhang, X. Li, L. Cheng, Y. Liu, and Y. Gao, "Power profile-based antenna selection for millimeter wave MIMO with an all-planar lens antenna array," *IEEE Access*, vol. 9, pp. 40476–40485, 2021, doi: 10.1109/ACCESS.2021.3064950.

[28] X. Meng, M. Nekovee, and D. Wu, "The design and analysis of electronically reconfigurable liquid crystal-based reflectarray metasurface for 6G beamforming, beamsteering, and beamsplitting," *IEEE Access*, vol. 9, pp. 155564–155575, 2021, doi: 10.1109/ACCESS.2021.3125837.

[29] J. A. Ganie and K. Saurav, "1-bit polarization rotating and beam-switching transmitarray for millimeter wave MIMO applications," *IEEE Access*, vol. 10, pp. 44945–44953, 2022, doi: 10.1109/ACCESS.2022.3170100.

[30] S. Li, Z. N. Chen, T. Li, F. H. Lin, and X. Yin, "Characterization of metasurface lens antenna for sub-6 GHz dual-polarization full-dimension massive MIMO and multibeam systems," *IEEE Trans. Antennas Propag.*, vol. 68, no. 3, pp. 1366–1377, Mar. 2020, doi: 10.1109/TAP.2020.2968849.

[31] Z. Wani, M. P. Abegaonkar, and S. K. Koul, "High-low-epsilon biaxial anisotropic lens for enhanced gain and aperture efficiency of a linearly polarized antenna," *IEEE Trans. Antennas Propag.*, vol. 68, no. 12, pp. 8133–8138, Dec. 2020, doi: 10.1109/TAP.2020.2983787.

[32] X. Zhong, L. Chen, Y. Shi, and X. Shi, "Design of multiple-polarization transmitarray antenna using rectangle ring slot elements," *IEEE Antennas Wireless Propag. Lett.*, vol. 15, pp. 1803–1806, 2016, doi: 10.1109/LAWP.2016.2537386.

JAVID AHMAD GANIE (Graduate Student Member, IEEE) received the B.Tech. degree in electronics and communication engineering from the Islamic University of Science and Technology, Jammu and Kashmir, India, in 2016, and the M.Tech. degree in electronics and communication engineering from Shri Mata Vaishno Devi University, Katra, Jammu and Kashmir, in 2019. He is currently pursuing the Ph.D. degree with the Department of Electrical Engineering, Indian Institute of Technology Jammu (IIT Jammu), Jammu and Kashmir. His research interests include the design of high-gain linearly and circularly polarized antennas, transmitarrays, and reflectarrays. He was a recipient of the prestigious Prime Minister's Research Fellowship (PMRF) which is awarded by the Ministry of Education, Government of India. He also serves as the Chair for the IEEE MTTS Student Branch Chapter, IIT Jammu.

KUSHMANDA SAURAV (Member, IEEE) received the B.E. degree in electronics and telecommunication from Bengal Engineering and Science University, Shibpur, India, in 2009, the M.Tech. degree in electronics and communication engineering from IIT Roorkee, India, in 2011, and the Ph.D. degree in electrical engineering from IIT Kanpur, India, in 2017. He was a Postdoctoral Fellow with the Royal Military College Canada. He is currently an Assistant Professor with the Department of Electrical Engineering, Indian Institute of Technology Jammu, India. He has experience supervising M.Tech. and Ph.D. students and undertaking sponsored projects. He has published more than 70 research papers in esteemed journals and conferences. His research interests include microwave and millimeter-wave antennas and frequency-selective surfaces. He has served as a Reviewer for IEEE, IET, and Wiley journals. He is actively involved in the professional activities of the IEEE. He is also the Faculty Advisor of the IEEE MTTS and the APS Student Branch Chapters of IIT Jammu.

• • •